10

Volume-of-Fluid (VOF) Simulations of Marangoni Bubbles Motion in Zero Gravity

Yousuf Alhendal and Ali Turan
The University of Manchester
United Kingdom

1. Introduction

This chapter deals with two-phase flows, i.e. systems of different fluid phases such as gas and liquid. A typical example of a two-phase flow is a motion of a particle (bubble or droplet) in a stagnant fluid (liquid or gas). In many branches of engineering it is important to be able to describe the motion of gas bubbles in a liquid (Krishna & Baten, 1999). In multiphase flow, the simultaneous flow strongly depends on the gravity force. However, in zero gravity conditions, buoyancy effects are negligible and as an alternative, three different methods were found to make the bubbles or drops move in zero gravity. They are electrocapillary, solutalcapillary and thermocapillary motion.

When a temperature gradient exists on the interface, the surface tension varies along the interface, resulting in bulk fluid motion, called thermocapillary (Marangoni) flow. In normal gravity this thermocapillary flow tends to be weighed down by buoyancy driven flow. However, for small geometry and/or zero gravity environments, this is not the case and thermocapillary is dominant and it could become an important driving force.

Bubbles suspended in a fluid with a temperature gradient will move toward the hot region due to thermocapillary forces. Surface tension generally decreases with increasing temperature and the non-uniform surface tension at the fluid interface leads to shear stresses that act on the outer fluid by viscous forces, thus inducing a motion of the fluid particle (a bubble or a drop) in the direction of the thermal gradient. In space, where buoyancy forces are negligible, thermocapillary forces can be dominant and can lead to both desirable and undesirable motion of fluid particles.

Particle dynamics has become a very important study area for fundamental research and applications in a zero gravity environment, such as space material science, chemical engineering, space-based containerless processing of materials e.g., glass is believed to have the potential of producing very pure materials, (Uhlmann, 1982), and thermocapillary migration may provide mechanisms to remove bubbles from the melt. Control of vapor bubbles forming in both the fuel systems of liquid-rockets (Ostrach, 1982) and the cooling system of space habitats may be achievable using thermocapillary migration. Thermocapillary migration may also lead to accumulation of gas bubbles on the hot surface of heat exchangers and reducing their efficiency. Ostrach (1982) studied various types of fluid flows that could occur under low-gravity conditions and pointed out that Marangoni convection is one of the important flows. In practical applications, it is frequently necessary

to deal with a large number of bubbles or drops and their collective behavior may differ from what one might expect based on results for a single particle.

1.1 The need for CFD in zero gravity investigation

An understanding of the behaviour of two phase fluids flow in zero gravity conditions is important for designing useful experiments for the space shuttle and the international space station. In addition, such understanding is important for the future design of thermo-fluid systems and machinery that might be employed in comparable environments. However, it is quite expensive and time-consuming to design and fabricate a space experiment and very little is known of the microgravity behavior of fluids due to the relative difficulty of obtaining experimental data under such conditions.

The available experimental results are usually supposed to be the major source of information on the behaviour of the physical process of two phase flow at zero gravity. However, because of the difficulties in obtaining experimental results, the numerical methods modelling turns out to be the ideal tool allowing to investigate the behaviour of two phase flow and capture the flow physics in plenty of time and of course less cost. The available literature of the zero gravity particle behavior is limited to low Re and Ma because of the difficulties in obtaining experimental results in microgravity (Kang et. al., 2008), and computer simulation can help understand the basic fluid physics, as well as help design the experiments or systems for the microgravity condition. Experiments under normal and microgravity conditions are too costly as well as being complicated, (Bozzano, 2009), and hence, numerical simulations become an important tool in research studies of two-phase flows under a microgravity environment. wolk et al, (2000) referred to the important of prediction of the flow pattern in a gas/liquid flow in two phase flow and especially concerning the particle dynamics in zero gravity and the need to predict accurately the existing flow patterns. A number of experiments have been conducted in drop towers, sounding rockets and aboard space shuttles; see the extensive review of (Subramanian et al., 2002). These experiments have noted complicated transients and time-dependent behavior in regimes where the flow has finite viscous and thermal inertia (Treuner et al., 1996; Hadland et al., 1999; Wozniak et al., 2001). Those experimental studies noted that there are no theoretical or numerical results with which to compare their experiments. It is also uneasy to get complete information about the behavior of bubble in space and a CFD study has been undertaken by many researchers to compare and analyse their experimental results, (Treuner et al., 1996). The shape and the area of the varying interface are very complex and a simulation study is required, (Subramanian et al., 2009). Two phase flow experiments generally require continuous observation of moving fluid during a test, which makes the experiment complicated. It is also a challenge for space researchers to design a space experiment to accommodate most of their objectives. For the above reasons and more it is necessary to carry out appropriate numerical simulations for the behavior of bubble/drop in microgravity and numerical simulation can help understand the basic fluid physics, as well as assist design the experiments or systems for the zero gravity environment.

In this chapter, we are specifically targeting the use of computation in order to simulate thermocapillary (Marangoni) fluid flow in a zero gravity condition to better understand the physical processes behind many of the observed physical phenomena of zero gravity environments. It also allows sensitivity and feasible studies to be carried out for different parameters and design.

1.2 Description of the chapter and objectives

In this chapter we will use the ANSYS-Fluent (Release13.0, 2011) code to analyze and design bubble flow system in a zero gravity environment and investigate sensitivity studies to various parameters.

The literature review of this chapter examines the challenges facing fluid experiments aboard orbiting spacecraft. This illustrates the importance of the CFD simulations and examines the effect of several external and internal forces on the bubble flow in zero gravity. The finite volume method (FVM) with a fixed non uniform spatial grid was used to computationally model 2-D axis-symmetric and 3-D domains. The model's solution algorithms, boundary conditions, source terms, and fluid properties used in the simulation are described in details in this chapter with sample calculation.

This chapter provides an interesting opportunity to test the capability of finite volume method (FVM) simulation and the Volume of fluid (VOF) method to accurately represent thermocapillary flow of single and multi bubbles. In addition, several published articles concerning the use of the Volume of Fluid (VOF) method in bubble/drops simulation are reviewed. Lastly, the simulation was able to examine scenarios not covered experimentally in order to verify the theoretical prediction of the effect of temperature different, column-particle aspect ratio, and effect of rotational on the coalescence of multi bubbles under the effect of both fluid rotation and surface tension. Though a huge amount of publications (textbooks, conference proceedings and journal articles) concern two-phase, publications on two phase flow in microgravity is a very little studied field and information about bubble behavior in a rotating column in particular is not so complete comparing with other physical phenomena in normal gravity. These are the main reasons for carrying out simulation research in microgravity.

2. Fluid dynamics

In order to study two-phase fluids in microgravity we should understand concepts and notions of fluid dynamics used in later sections and to remind the reader of some fundamental dimensionless quantities which will be frequently encountered.

2.1 Compressible and incompressible fluid

Fluids are compressible if changes in pressure or temperature will result in changes in density. However, in many situations the changes in pressure and temperature are sufficiently small that the changes in density are negligible. In this case the flow can be modeled as an incompressible flow.

2.2 Newtonian flow

Sir Isaac Newton showed how stress and the rate of strain are related for many common fluids. The so-called Newtonian fluids are described by a coefficient called viscosity, which depends on the specific fluid.

2.3 Viscosity

Viscosity describes fluids resistance to flow and may be thought as a measure of fluid friction. In viscous problems fluid friction has significant effects on the fluid motion. Real fluids are

fluids which have a resistance to shear stress. Fluids which do not have any resistance are called ideal fluid. Viscosity is divided in two types: dynamic (or absolute) and kinematic viscosity. Dynamic viscosity is the ratio between the pressure exerted on the surface of a fluid and the velocity gradient. The SI physical unit of dynamic viscosity is Pa.s. In many situations, we are concerned with the ratio of the viscous force to the inertial force, the latter characterized by the fluid density ρ. This ratio is characterized by the kinematic viscosity, defined as follows:

$$\nu = \frac{\mu}{\rho} \tag{1}$$

Where v is the kinematic viscosity in m^2/s, ρ is the density and μ is the dynamic viscosity.

2.4 Reynolds number

The Reynolds number is a measure of the ratio of inertial to viscous forces and quantifies the importance of these two types of forces for given flow conditions. It is the most important dimensionless number in fluid dynamics and it is commonly used to provide a criterion for determining dynamic similitude. Reynolds number is defined as follows:

$$\mathrm{Re} = \frac{Vo\ R}{\mathrm{v}} \tag{2}$$

Where R is the particle radius in m, V_o is the velocity in m/s.

The velocity $V_o$derived from the tangential stress balance at the free surface is used for scaling the migration velocity in Eq. (2) and (4):

$$V_0 = \frac{\frac{d\sigma}{dt}\frac{dT}{dx}}{\mu} \tag{3}$$

Where, the constant $\frac{d\sigma}{dT}$(or σ_T) is the rate of change of interfacial tension and $\frac{dT}{dX}$, the temperature gradient imposed in the continuous phase fluid.

2.5 Marangoni number

In zero gravity a bubble or a drop in an immiscible fluid will move toward the warmer side when subjected to a temperature gradient. Such a phenomenon is known as Marangoni flow or the thermocapillary migration. Marangoni flow is induced by surface tension gradients asa result of temperature and/or concentration gradients.

$$Ma = \frac{R V_0}{\alpha} = \mathrm{Re.Pr} \tag{4}$$

Here, α is the temperature diffusivity

2.6 Prandtl number (Pr)

Pr is the ratio of kinematic viscosity to thermal diffusivity. Very high Pr (Pr >> 1) fluids are usually very viscous, while highly thermally conducting fluids, usually liquid metals, have low Pr (Pr << 1).

$$\Pr = \frac{\nu}{\alpha} \tag{5}$$

In 1959, Young et al. (1959) first investigated the thermocapillary migration of bubbles and drops with their linear model, which is suitable for small Reynolds number (Re) and small Marangoni number (Ma). This model is now called the YGB model. The Reynolds number is the ratio of inertial forces to viscous forces. Small Re means that inertial effects are negligible. The Marangoni number is the ratio of convective transport of energy to heat conduction. Small Ma means that convective heat transfer is negligible compared to heat conduction. YGB model velocity V_{YGB} (Young et al. 1959) is expressed as follows:

$$V_{YGB} = \frac{2\left|\sigma_T\right| R\nu\Delta T_\infty}{(2\mu + 3\mu')(2k + k')} \tag{6}$$

where R is the radius of the bubble; $\Delta T\infty$ is the temperature gradient; μ and μ' , k and k' are the dynamic viscosity, thermal conductivity of gas and continuous phase, respectively.

2.7 Microgravity

Gravity is a force that governs motion throughout the Universe. It holds us to the ground, keeps the Moon in orbit around the Earth, and the Earth in orbit around the Sun. The nature of gravity was first described more than 300 years ago. Gravity is the attraction between two masses. Bigger the mass, most apparent the attraction is. The acceleration of an object caused only by gravity, near the surface of the Earth, is called normal gravity, or 1g. The condition of microgravity comes about whenever an object is in "free fall": that is, it falls faster and faster, accelerating with exactly the acceleration due to gravity (1g). Objects in a state of free-fall or orbit are said to be "weightless."

3. Computational procedure

3.1 VOF model

The CFD software offer several models to incorporate multiphase flows; every model is developed for its own specific flow type. The governing continuum conservation equations for two phase flow were solved using the commercial software package (ANSYS, 2011), and the Volume of Fluid (VOF) method (Hirt et al. 1981) was used to track the liquid/gas interface.

Volume of Fluid (VOF) model is designed for two or more immiscible fluids, where the position of the interface between the fluids is of interest (ANSYS, 2011). Applications of the VOF model include the prediction of jet break-up, the motion of large bubbles in a liquid, the motion of liquid after a dam break, or the steady or transient tracking of any liquid-gas interface and If the bubble is so large that it extends across several control volumes, the VOF formulation is appropriate to track its boundary. Most ANSYS-FLUENT models are available in combination with the VOF model. For example, the sliding-mesh model can be used to predict the shape of the surface of a liquid in a mixing tank. The deforming mesh capability is also compatible with the VOF model. The porous media model can be used to track the motion of the interface between two fluids through a packed bed or other porous region. The effects of surface tension may be included (for one specified phase only), and in combination with this model, you can specify the wall adhesion angle. Heat transfer from

walls to each of the phases can be modeled, as can heat transfer between phases. The basic idea of the volume of fluid (VOF) method is to consider a colour function, defined as the volume fraction of one of the fluids within each cell, to capture the interface. This function will be one if the cell is filled with the gas phase, zero if the cell is filled with the liquid phase, and between zero and one in the cells where there is an interface. The VOF method belongs to the so called "one" fluid method, where a single set of conservation equations is solved for the whole domain. The VOF method codes have been used extensively to calculate the hydrodynamics of bubbles rising in liquid by Kawaji et al.,(1997). They noted a new result which was not observed experimentally when they compared the numerical simulation results from a two dimensional simulation of a Taylor bubble rising in a stagnant liquid filled tube to experimental analysis. The work of Tomiyama et al., (1993) illustrated the capability of VOF to accurately simulate bubble shape, and the simulated shapes were shown to agree with experimental published data. The researchers showed their results of predicted bubble shapes were in good agreement with those of Bhaga & Weber (1981). The VOF simulations with gas-liquid systems could be used as an investigative tool for studying bubble rise and bubble-bubble interactions in gas-liquid bubble columns, (Alhendal et al.,2010). The Volume of Fluid (VOF) method is made for flows with completely separated phases; the phases do not diffuse into each other (ANSYS, 2011). "geo-reconstructed-VOF" method in Fluent is chosen for this investigation. Geo-reconstruction is added to the VOF scheme to define the free surface more accurately, (Hirt et al., 1981). Applications of the VOF model include stratified flows, free-surface flows, the steady or transient tracking of any liquid gas interface (ANSYS, 2011).

3.2 Formulation of the problem and the solution strategy

The movement of the gas–liquid interface is tracked based on the distribution of α_G, the volume fraction of gas in a computational cell, where $\alpha_G = 0$ in the liquid phase and $\alpha_G=1$ in the gas phase. Therefore, the gas–liquid interface exists in the cell where α_G lies between 0 and 1. The geometric reconstruction scheme that is based on the piece linear interface calculation (PLIC) method of Youngs (1982) is applied to reconstruct the bubble free surface. A single momentum equation, which is solved throughout the domain and shared by all the phases, is given by:

$$\frac{\partial}{\partial t}(\rho\vec{v}) + \nabla.(\rho\vec{v}\vec{v}) = -\nabla p + \nabla.[\mu(\nabla\vec{v} + \nabla\vec{v})^T] + \rho + \vec{F} \tag{7}$$

where v is treated as the mass-averaged variable.

$$v = \frac{\alpha_G\rho_G v_G + \alpha_L\rho_L v_L}{\rho} \tag{8}$$

In this bubble simulation, $\vec{F}$ represents the volumetric forces at the interface resulting from the surface tension force per unit volume. The CSF model of Brackbill et al., (1992) was used to compute the surface tension force for the cells containing the gas–liquid interface:

$$\vec{F} = \sigma\frac{\rho kn}{\frac{1}{2}(\rho_L + \rho_G)} \tag{9}$$

Where σ is the coefficient of surface tension, n is the surface normal which is estimated from the gradient of volume fraction, κ is the local surface curvature calculated as follows:

$$k = -(\nabla \hat{n}) = \frac{1}{n}\left[\frac{n}{|n|}\nabla|n| - (\nabla . n)\right] \tag{10}$$

The tracking of the interface between the gas and liquid is accomplished by the solution of a continuity equation for the volume fraction of gas, which is:

$$\frac{\partial}{\partial t}(\alpha_G \rho_G) + \nabla \cdot (\alpha_G \rho_G \vec{v}_G) = 0 \tag{11}$$

The volume fraction equation is not solved for the liquid; the liquid volume fraction is computed based on the following constraint:

$$\alpha_G + \alpha_L = 1 \tag{12}$$

where α_G and α_L is the volume fraction of gas and liquid phase respectively.

The properties appearing in the transport equations are determined by the presence of the component phases in each control volume and are calculated as volume-averaged values. The density and viscosity in each cell at interface were computed by the application of following equations:

$$\rho = \alpha_G \rho_G + (1 - \alpha_G)\rho_L \tag{13}$$

$$\mu = \alpha_G \mu_G + (1 - \alpha_G)\mu_L \tag{14}$$

where ρ_G, ρ_L, μ_G and μ_L is density and viscosity of gas and liquid phase respectively, while α_G is the volume fraction of gas. The energy equation is also shared among the phases:

$$\frac{\partial}{\partial t}(\rho E) + \nabla . [\vec{v}(\rho E) + p)] = \nabla . (\kappa_{eff} \nabla T) \tag{15}$$

The VOF model treats energy, E, and temperature, T, as mass-averaged variables:

$$E = \frac{\sum_{q=1}^{n} \alpha_q \rho_q E_q}{\sum_{q=1}^{n} \alpha_q \rho_q} \tag{16}$$

where E_q for each phase is based on the specific heat of that phase and the shared temperature. The effective thermal conductivity k_{eff} is also shared by the phases.

3.3 Using Fluent - Grid generation and independence

The bubble was initially placed at the centre of the cylindrical domain by using the region adaptation option of ANSYS-Fluent. To do that, a spherical patch or domain was selected at

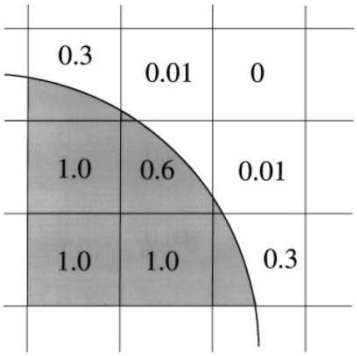

Fig. 1. Volume of fluid (VOF) interface reconstruction

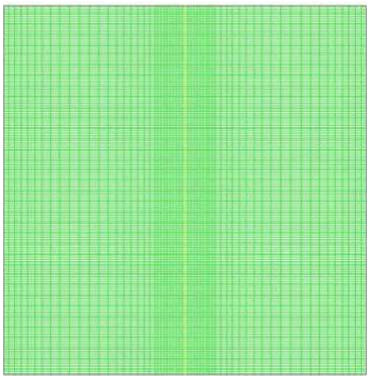

Fig. 2. Typical mesh used for Marangoni cases

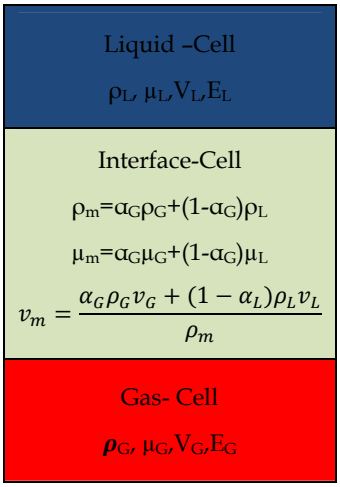

Fig. 3. Volume fraction and properties in each cell in the bubble

the cylinder with void fraction of 1. The rest of the cylindrical domain was specified as liquid, i.e., with a void fraction of zero. Figure 4 depicts the bubble inside the computational domain at the initiation of a simulation. The geometry of the two-dimensional model is somewhat similar to the one used by Thompson et al. (1980), and extension to fully 3-dimensional model is followed by the 2-dimensional study. The initial rise velocity for the bubble was zero. The upper surface of the fluid is a hooter than the bottom surface boundary, which is assumed to be flat with no-slip walls. The grid details are shown in fig. 2. After doing the required sensitivity grid tests, a non-uniform grid of 7200 cells was used throughout the 2-D axis simulations with the grid lines clustered towards the centre, and uniform grid of 372000 cells for the 3-D cases.

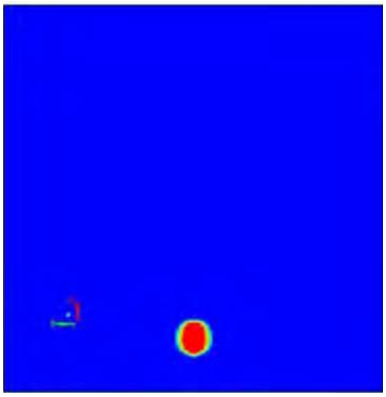

Fig. 4. Initial condition for the bubble inside the 2-D axis.

3.3.1 Grid independence

For the 2-d axis, the domain was split into two areas to create non-uniform mesh clustered in the area of interest (centre), see fig. 2 for domain mesh technique. Another important point is that, when using the axisymmetric solver, you create a mesh only for the half of your domain, thus reducing drastically the number of cells you use, and consequently the time of calculation. Fluent will accept the axis in the direction of the positive X-axis only. The model was verified for grid independence and geometry-related such as 2-d axis and rotational periodic flow as shown in figs. 5 & 6. Grid independence was examined by using three grid systems with 20x20x80 (96000 cells), 30x30x120 (324000 cells) and 40x40x160 (768000 cells). The three simulations showed nearly bubble migration for the simulations with the maximum difference of less than 1% between the cases. For calculation efficiency, it was found that the 30x30x120 mesh produces a grid-independent solution and was used in this calculation with 0.001 time step. For some cases when using the periodic flow solver, you create a mesh only for the quarter, half, three quarters of the domain, thus reducing the number of cells you use, and consequently the time of calculation. Periodic boundary condition is recommended for the bubble located at the centre of the domain.

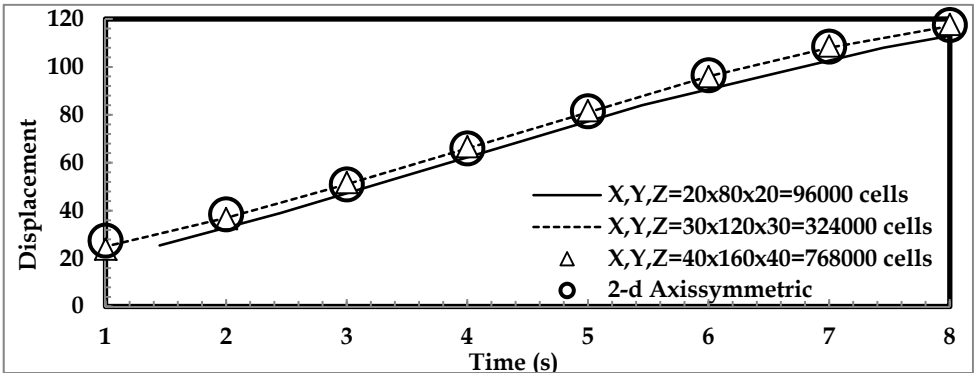

Fig. 5. Grid independence shows identical bubble migration for 2-d axis & 3-D simulations

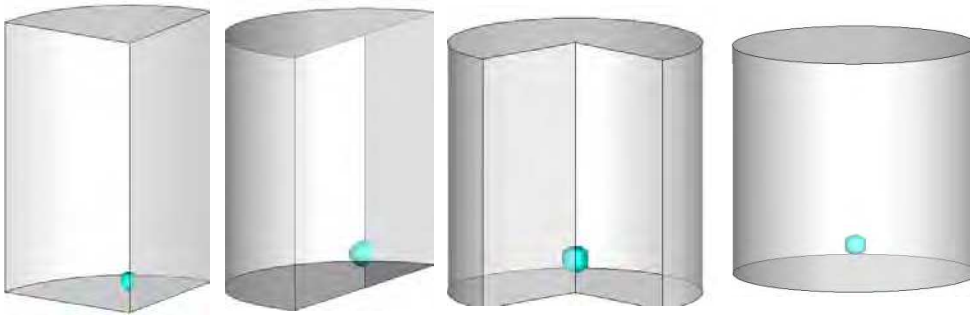

Fig. 6. Rotational periodic/full geometry used to calculate bubbles/drops migration

4. Numerical procedure and simulation

In this first test case, a bubble with a diameter of 6 mm was placed 10 mm from the bottom wall (cold). Hence, the size of the computational wall bounded domain was chosen as 120 x60 mm with no "inflow or overflow" from the sides. For the purposes of these simulations, ethanol properties were taken to be same as the properties given in table (1) from Thompson et al. (1980). The unsteady 2-D axisymmetric and 3-D models were formulated using the commercial software package (ANSYS-FLUENT® v.13, 2011) in modeling the rise of a bubble in a column of liquid in zero gravity (Marangoni flow). Surface tension and its temperature coefficient used in the simulations for the ethanol and N_2 are (σ =27.5 dynes/cm and σ_T =-0.09 dynes/cm°C), (Kuhlmann, 1999). A numerical prescription for the surface tension vs. temperature behavior is provided via a user defined function (UDF) which can be dynamically linked with the FLUENT solver.

	Unit	Ethanol	Nitrogen (N_2)
Density (ρ)	kg/m^3	790	1.138
Specific Heat (Cp)	j/kg-k	2470	1040.7
Thermal Conductivity (k)	w/m-k	0.182	0.0242
Viscosity (μ)	kg/m-s	0.0012	1.66e-5
Surface tension coefficient (σ_T)	w/m.k	0.00009	----
Velocity V_O Eq. (3)	(m/s)	0.075	
Velocity V_{YGB} Eq. (6)	(m/s)	0.034	
Velocity –V (CFD)	(m/s)	0.014	
Scaled velocity V/ V_{YGB}	-	0.41	
Prandtl Number (Pr)	Eq. (5)	16.28	
Reynolds Number(Re)	Eq. (2)	197.5	
Marangoni Number(Ma)	Eq. (4)	3216.4	

Table 1. Physical properties of the liquids employed in the simulation at 300K and sample results for bubble diameter= 9 mm for (Pr=16.28).

4.1 Description of test cases and results

Predicted simulations have been compared with the experimental work of Thompson et al., (1980) as shown in fig. 8 and agreement obtained. In a non-uniform temperature gradient, the fluid on the bottom is cold, and therefore has greater surface tension. The fluid on the top is hot, therefore possesses weaker surface tension. The tendency of the fluid with greater surface tension is going to pull the fluid with less surface tension towards it. This motion would be from top to bottom. "Whenever surface is created, heat is absorbed, and whenever surface is destroyed heat is given off. Therefore a swimming bubble absorbs heat at its hot end and rejects heat at its cold end" (Nas & Tryggvason, 1993) as seen in temperature contour of fig 9.

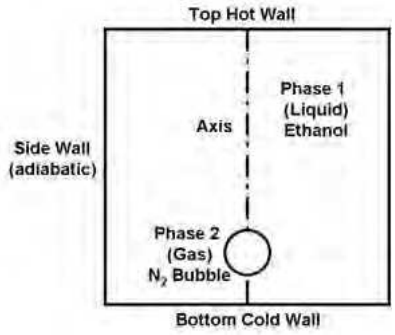

Fig. 7. Schematic of bubble migration in a uniform temperature gradient.

The ANSYS-FLUENT code allows for the use of different gravity values. With this option, we ran several cases for different geometry conditions. The cases that are presented in this chapter were conducted in a zero gravity environment so that the flow would be driven by surface tension instead of buoyancy. On earth-based, where gravity presents, the flow is mainly driven by buoyancy, and most of its effects have already been studied. On the other hand, surface tension driven flows have not been studied to such a high level and this was an opportunity to do so.

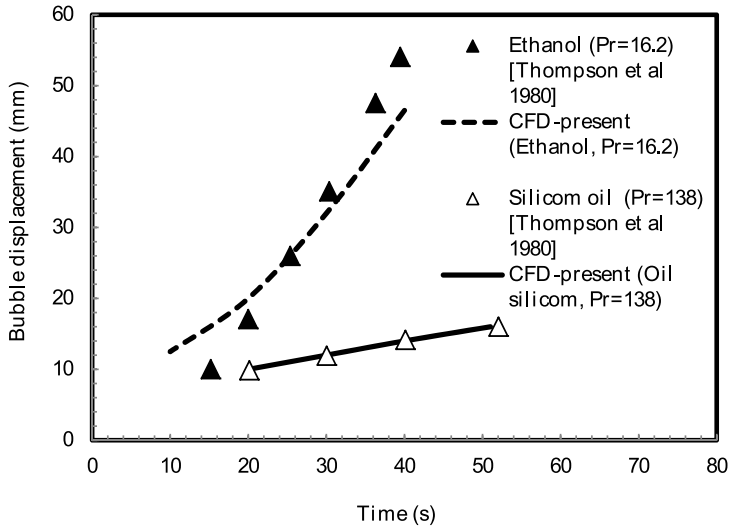

Fig. 8. Result validation of present-CFD calculation with (Thompson et al., 1980) for N2 = 6mm diameter

4.2 Effect of liquid temperature upon bubble migration

The second test case in this chapter is the most representative and interesting case. For this test case the linear temperature distribution was used between the walls. As we ran and visualized these cases we interpreted how they affected the bubble migration speed toward the hotter side. Fig. (9) shows that the different temperature differences between the walls made the bubble move faster for greater temperature differences, or slower for small temperature differences. For the design fluid, Ethanol in this case, hotter side temperature above 330K will not have significant effect on the bubble speed and less than 320K possibly will not move the bubble. With these concepts in mind we selected a temperature range vary from (320-335) K for the top wall and 300K was fixed for the bottom wall. With these design concepts we started to set boundary conditions and to slightly change some initial conditions. All these cases gave us insight on the behavior of such a temperature differences. In these test cases simulations of bubble thermocapillary migration, Re and Ma range from 228.6 to 274.3 and from 3722.7 to 4467.3, respectively. Sensitivity tests results for different bulk liquid temperatures in figures 9 and 10 show the capability of ANSYS-Fluent to simulate two phase flow in microgravity environment using VOF model.

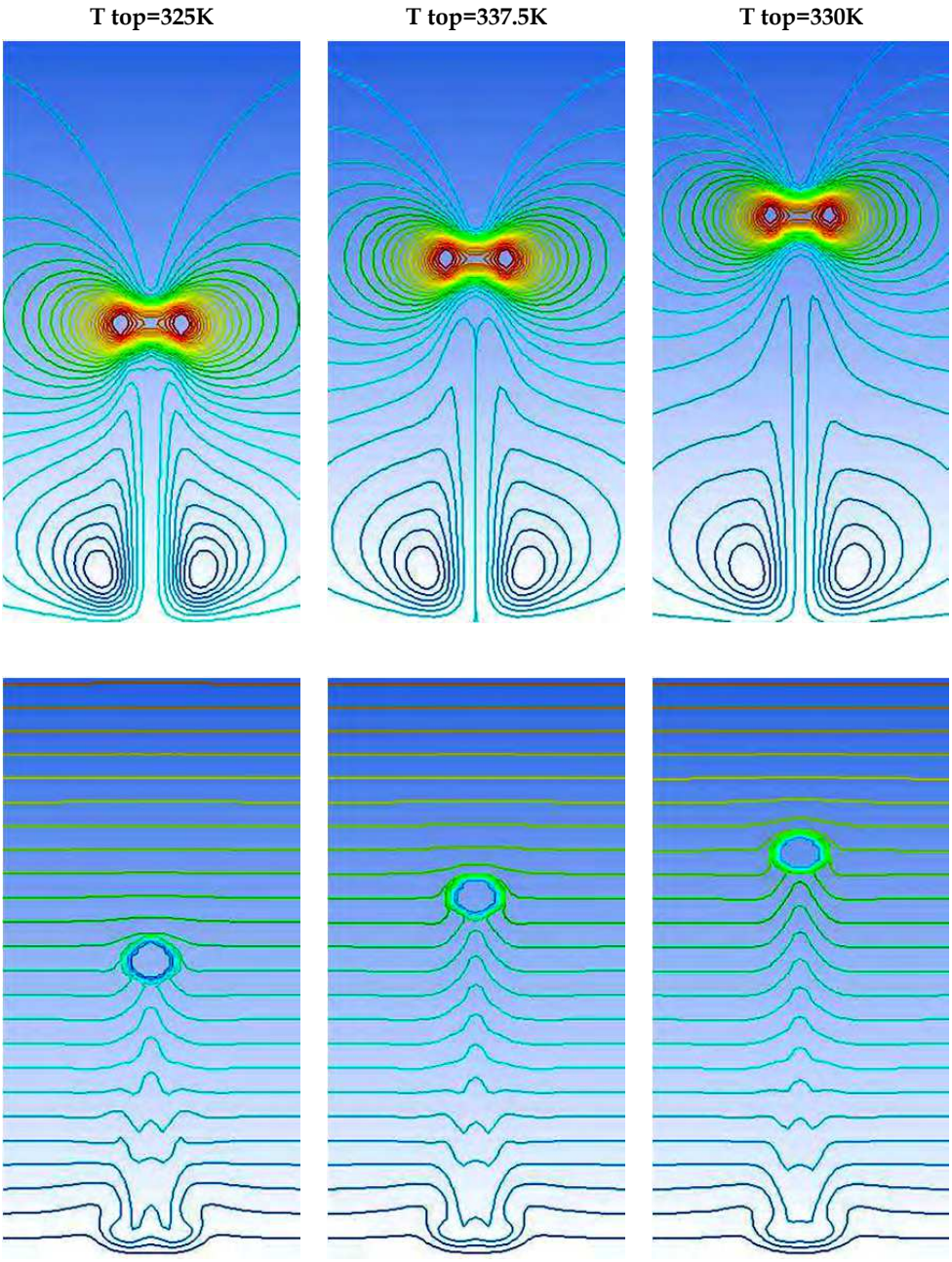

Fig. 9. Temperature contours (bottom) and streamlines (top) for the single bubble (d=10 mm) at t=5 s.

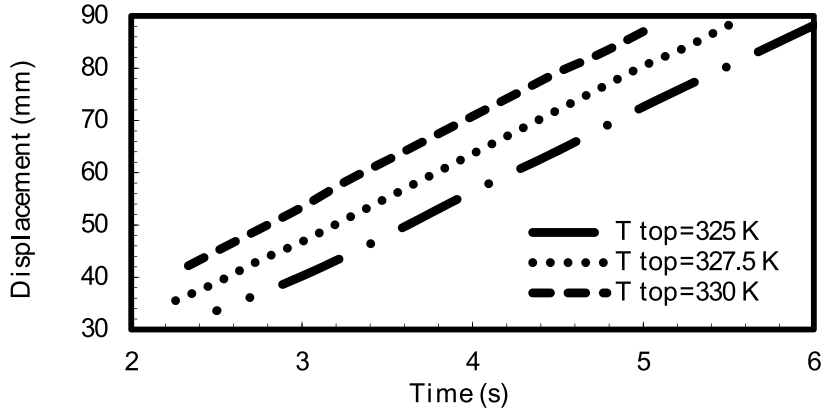

Fig. 10. Sensitivity tests results for different bulk liquid temperatures (Pr=16.3) at time (t)=5 second, and bubble diameter (d) for N2 =10 mm

4.3 Effect of aspect ratio upon bubble migration

We report the results of an extensive numerical investigation on the speed of rise of gas bubbles diameters in the size range of 4-10 mm in stagnant Ethanol liquid in a column with diameters of 20, 40, 60, 80 mm. The column diameter was found to have a significant effect on the rise velocity of the bubbles as shown in fig. 11 below.

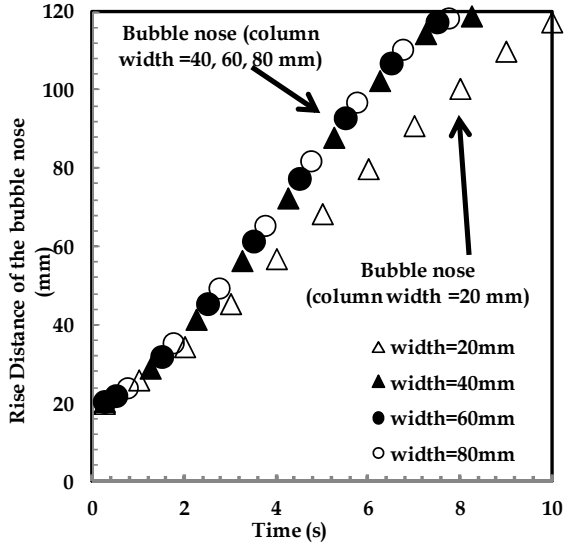

Fig. 11. Compares the x-coordinates of the nose of 10 mm bubbles rising in columns of 20, 40, 60, and 80 mm diameters

Figure 11 shows the effect of the column width on the raise speed of the bubble. The liquid phase stream lines profiles for three simulations is illustrated in figure 12. Figure 13 shows when the Aspect Ratio (AR) of the bubble diameter to the column diameter, is smaller than 0.355 the influence of the column diameter on the rise velocity is negligible. With increasing AR there is a significant reduction of the rise velocity.

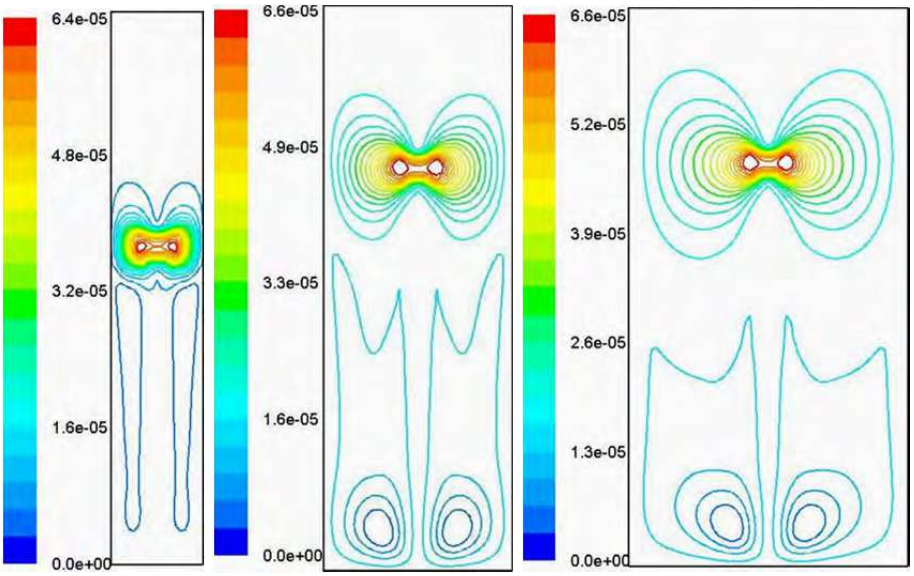

Fig. 12. CFD simulation for studies on rise velocity of single bubble in side a column AR=(0.5, 0.25, 0.1667) from the left to the right.

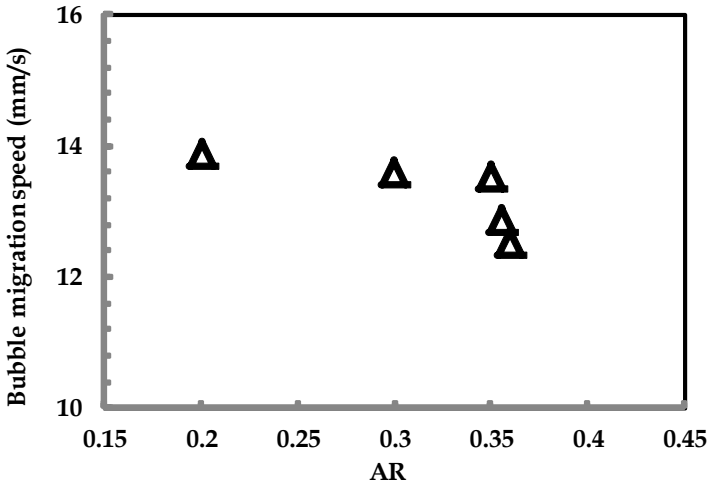

Fig. 13. Shows the effect of (AR) on the rise speed of single bubble

4.4 Effect of rotating cylinder upon bubble coalescence

In a rotating field, fluid particles which are less dense than the surrounding media migrate inward toward the axis of rotation (Annamalai et al. 1982). The results of three dimension rotating cylinder can complement the previous study in providing techniques for causing small bubble to move or bringing several unmovable small bubbles within a cylinder to coalesce into a large bubble which might subsequently be extracted or otherwise manipulated within the cylinder. The same technique can be used in glass melts processing. Under such conditions, rotation of the melt, followed by thermocapillary migration of the coalesced bubbles results in a "centrifugal fining" operation for bubble removal (Annamalai et al. 1982).

The effect of both cylindrical rotation and surface tension on the trajectory of the single bubble is illustrated in figure 12. In this figures, it can be seen that the angular velocity (ω) pulled the bubble towards the centre of rotation, and at the same time Marangoni force moved the bubble towards the hotter side.

As the cylinder begins to rotate from (5-50 rpm), the linear movement of the bubble changes and the bubble starts moving further towards the axis of rotation (centre). Results show that by adjusting the rotational speed, it is possible to change the gas bubble behavior in a thermocapillary flow. The results can help determine the new migration time and speed in the rotating cylinder. Figs 15-16 show that the transient development of the radial migration of the three bubbles will move from the rest towards the centre of the cylinder and towards the top side (hotter side). This movement depends on the angular speed (ω) and thermocapillary flow. These figures illustrate that bubble breakage and agglomeration can be controlled

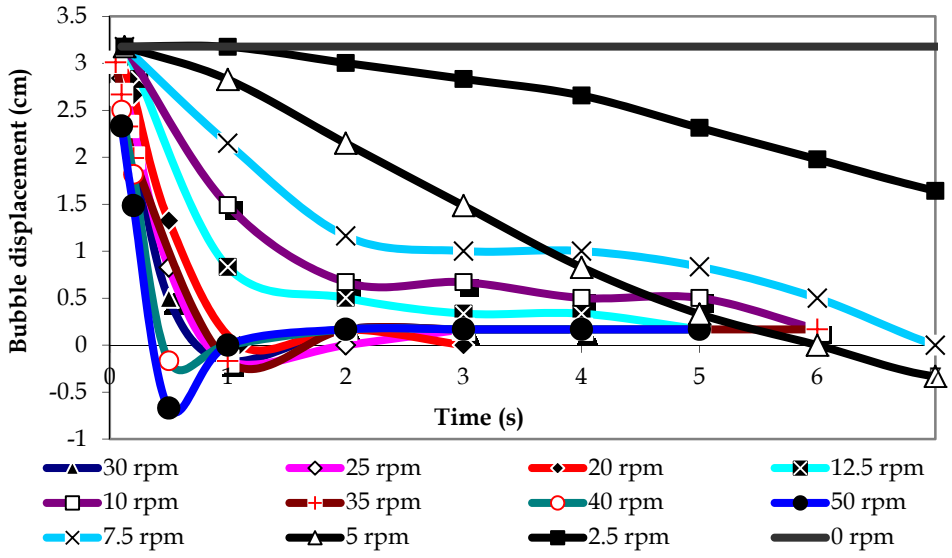

Fig. 14. Bubble displacement (cm) from the releasing position (3 cm from the axis of rotation) toward the axis of rotation and the hotter side (Marangoni)

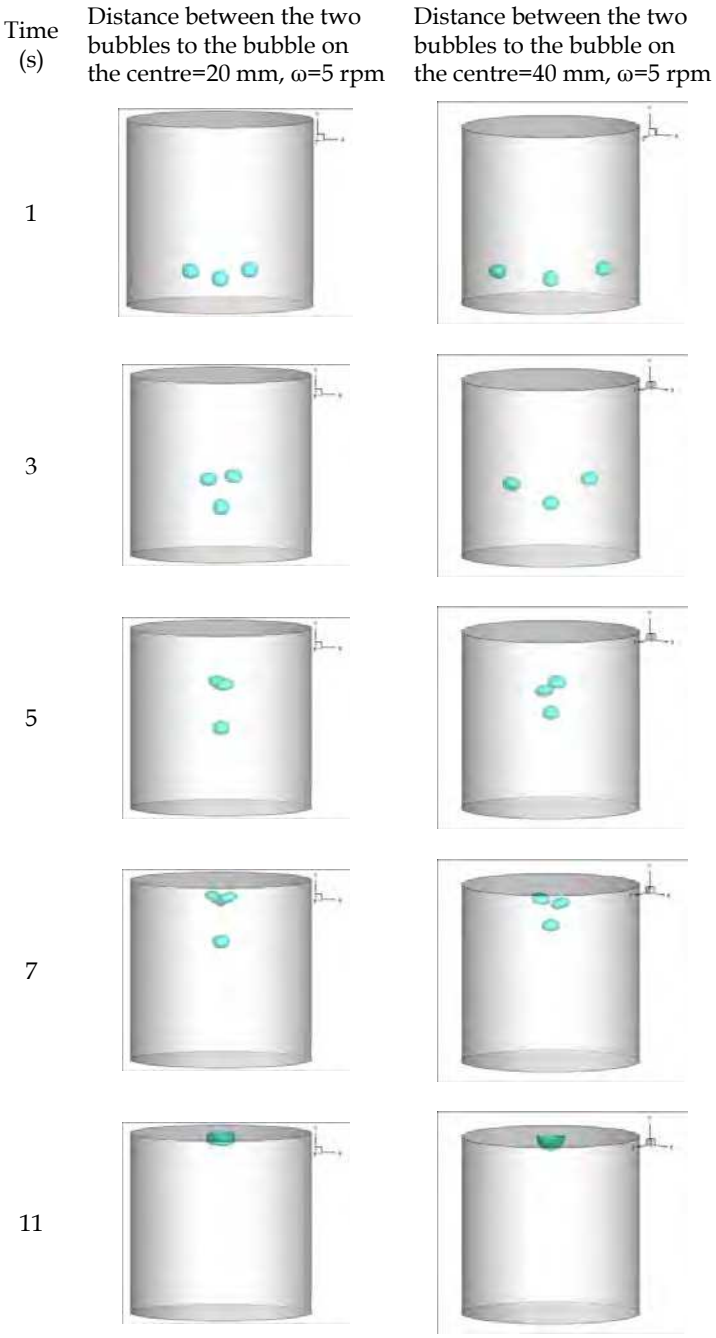

Fig. 15. Shows the coalescence sequence of 10 mm diameter bubbles

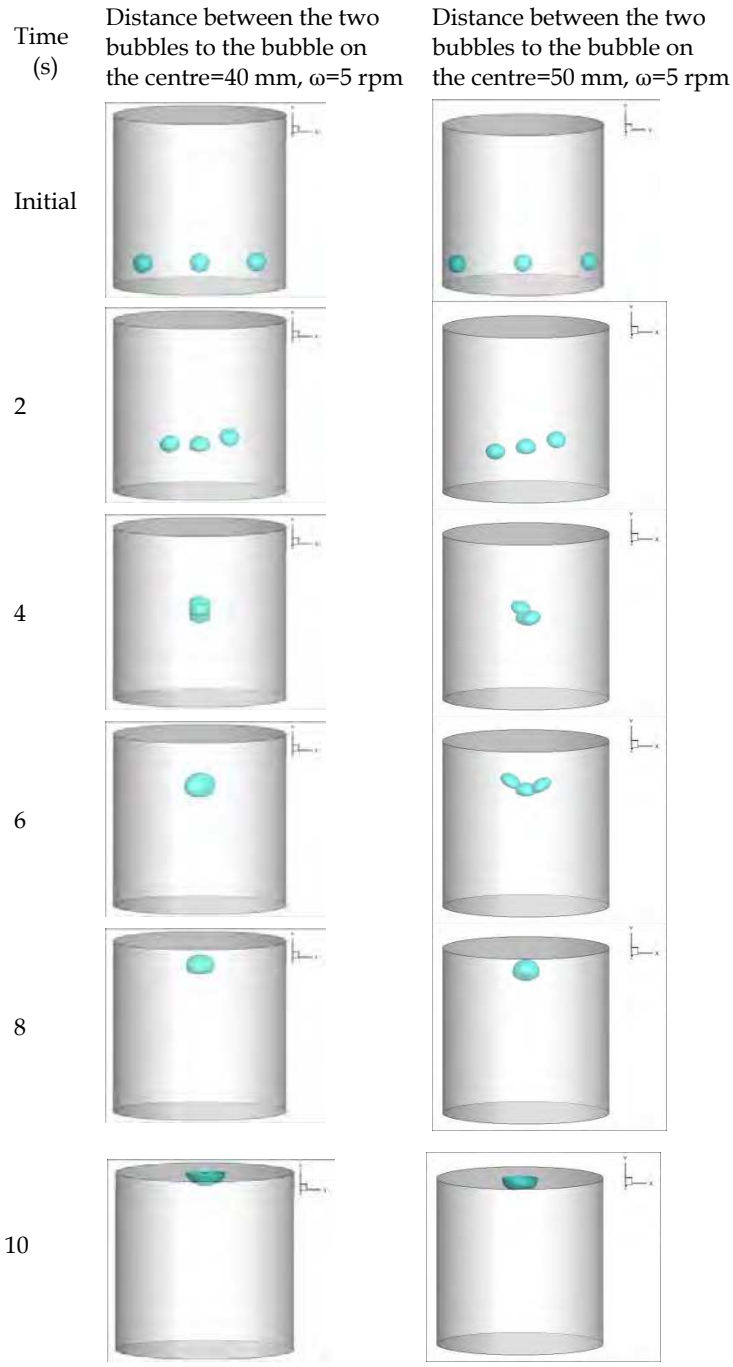

Fig. 16. Shows the coalescence sequence of 12 mm diameter bubbles

5. Conclusions and future work

In This chapter, it was shown by figures the conclusive existence of Marangoni bubble flow phenomena in a zero gravity environment. We discovered the effect of temperature, wall aspect ratio, and rotating cylinder on the bubble behavior at zero gravity using ANSYS 13. It has been proven that VOF is a robust numerical method for the simulation of gas-liquid two-phase flows, and the ability to simulate surface tension as a function of temperature (thermocapillary flow) using a UDF is possible for routine design and development engineering activities

A constant angular speed (ω) was applied to the walls of the cylinder which imparts an extra radial forced vortex motion to the adjacent fluid layer, the effect of which translates as a velocity towards the axis. The 3D simulation was complemented to the previous axissymmetry cases in providing techniques for bringing several unmovable small bubbles within a cylinder to coalesce into a large bubble or to its centre which might subsequently be extracted or otherwise manipulated within the cylinder. These results can help in determine the new migration speed and behavior of gas bubbles by adjusting the angular speed.

Most experimental in microgravity are limited to the case of shortage in time and some other space limitations. Computer simulations, on the other hand, are not restricted to such circumstance, and any arbitrary geometry can be simulated in addition to rotating system. Thanks to the increasing computer power, it is nowadays possible to solve more complex multiphase models. With that the computer solution proves to be a valuable tool to study the complex problem under the conditions of zero and reduced gravity, and from the results of this chapter we can see the ability of ANSYS-Fluent code to simulate Marangoni 3-d cases.

The behavior of the compound rotational and surface tension driven motion, shapes, and trajectories of bubbles is a new area of study, and it is planned to help support research area based on space applications. According to our knowledge, the present study 3-D-VOF-based method for simulating the influence of both rotational and thermocapillary on single and multi bubbles located off centre is first numerical study case in this field and no comparable investigation has been published in the open literature due to difficulty for researchers to access to microgravity facilities. In the future, more detail discussions for different breakage and coalescence times for a group of bubbles will be investigated and used to make kernels function which can be used in population balance equations.

6. References

Alhendal, Y.; Turan A. & Wael A. (2010). VOF Simulation of Marangoni Flow of Gas Bubbles in 2D-axisymmetric Column. Lecture Notes in Computer Science. Vol. 1. Issue 1. 673-680. May. DOI: 10.1016/j.procs.2010.04.072

Annamalai P., Shankar N., Cole R., & Subramanian R.S. (1982). Bubble Migration Inside a Liquid Drop in a Space Laboratory, Appl. Sci. Res., 38, 179-186

ANSYS-Fluent (2011). Users Guide.

Bhaga, T. & Webber, M. (1981). Bubbles in viscous liquids: shapes, wakes and velocities. J. Fluid Mech. 105, 61–85

Bozzano, G. & Dente M., (2009). Single bubble and drop motion modelling. AIDIC Conference Series, 09, 53-60 D01:10.3303/ACOS0909007

Hadland, P. H., Balasubramaniam, R., Wozniak, G. & Subramanian, R. S. (1999). Thermocapillary migration of bubbles and drops at moderate to large Marangoni number and moderate Reynolds number in reduced gravity. Expt. Fluids 26,240-248.

Hirt, C. & Nichols, B., (1981). Volume of Fluid (VOF) Method for the Dynamics of Free Boundaries. J. of Comp. Physics, 39, 201-225.

Kang, Q., Cui H. L., Hu L., & Duan L., (2008). On-board Experimental Study of Bubble Thermocapillary Migration in a Recoverable Satellite, Microgravity Sci. Technol (2008) 20:67 – 71-DOI 10.1007/s12217-008-9007-6

Kawaji, M., DeJesus, J.M., & Tudose, G., (1997). Investigation of Flow Structures in Vertical

Krishna, R. & J. M. van Baten, (1999). Rise Characteristics of Gas Bubbles in a 2D Rectangular Column: VOF simulations vs Experiments. International Communications in Heat and Mass Transfer 26, 965-974

Kuhlmann H.C., (1999). Thermocapillary Convection in Models of Crystal Growth, 152, Springer, Berlin, Heidelberg Springer Tracts in Modern Physics.

Nas, S. & Tryggvason, G. (2003). Thermocapillary interaction of two bubbles or drops.Int. J. Multiphase Flow 29, 1117-1135.

Ostrach, (January 1982). Low-Gravity Fluid Flows Annual Review of Fluid Mechanics,Vol. 14: 313-345-DOI: 10.1146/annurev.fl.14.010182.001525

Slug Flow", Nuclear Engineering and Design, Vol. 1 75, pp. 37-48

Subramanian, K., Paschke S., Repke JU, & Wozny G., (2009). Drag force modelling in CFD simulation to gain insight of packed columns, AIDIC Conference Series, 09, 299-308 D01:10.3303/ACOS0909035

Subramanian, R. S., Balasubramaniam, R. & Wozniak, G. (2002). Fluid mechanics of bubbles and drops. In Physics of Fluids in Microgravity (ed. R. Monti), pp. 149-177. London: Taylor and Francis.

Thompson, R.L., DeWITT, K.J. & Labus, T.L., (1980). Marangoni Bubble Motion Phenomenon in Zero Gravity,Chemical Engineering Communications 5 299-314.

Treuner, M., Galindo, V., Gerbeth, G., Langbein, D. & Rath, H. J. (1996). Thermocapillary bubble migration at high Reynolds and Marangoni numbers under low gravity. J. Colloid Interface Sci. 179, 114-127.

Uhlmann, D.R., (1982). Glass Processing in a Microgravity Environment. Materials Processing in the Reduced Gravity Environment of Space, Edited by Rindone, G.E., Elsevier, NY, USA, 269—278.

Wolk, G., M. Dreyer & H.J. Rath, (2000). Flow Pattern in Small Diameter Vertical Non-circular Channels. International Journal of Multiphase Flow, Vol. 26, pp. 1037-1061

Wozniak, G., Balasubramaniam, R., Hadland, P. H. & Subramanian, R. S. (2001). Temperature fields in a liquid due to the thermocapillary motion of bubbles and drops. Expt. Fluids 31, 84-89.

Young, N. O., Goldstein, J. S. & Block, M. J. (1959). The motion of bubbles in a vertical temperature gradient. J. Fluid Mech. 6, 350-356.

Youngs, D.L., (1982). Time-dependent multi-material flow with large fluid distortion. Numerical Methods for Fluid Dynamics, eds. K.W. Morton & M.J. Baines, Academic Press, pp. 273–285, Brackbill, J. U., Kothe, D. B. and Zemach, C., 1992, A continuum method for modeling surface tension, J.Comp. Physics 100, 335.

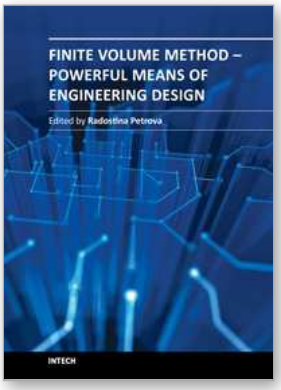

Finite Volume Method - Powerful Means of Engineering Design
Edited by PhD. Radostina Petrova

ISBN 978-953-51-0445-2
Hard cover, 370 pages
Publisher InTech
Published online 28, March, 2012
Published in print edition March, 2012

We hope that among these chapters you will find a topic which will raise your interest and engage you to further investigate a problem and build on the presented work. This book could serve either as a textbook or as a practical guide. It includes a wide variety of concepts in FVM, result of the efforts of scientists from all over the world. However, just to help you, all book chapters are systemized in three general groups: New techniques and algorithms in FVM; Solution of particular problems through FVM and Application of FVM in medicine and engineering. This book is for everyone who wants to grow, to improve and to investigate.

How to reference
In order to correctly reference this scholarly work, feel free to copy and paste the following:

Yousuf Alhendal and Ali Turan (2012). Volume-of-Fluid (VOF) Simulations of Marangoni Bubbles Motion in Zero Gravity, Finite Volume Method - Powerful Means of Engineering Design, PhD. Radostina Petrova (Ed.), ISBN: 978-953-51-0445-2, InTech, Available from: http://www.intechopen.com/books/finite-volume-method-powerful-means-of-engineering-design/volume-of-fluid-vof-simulations-of-marangoni-bubbles-motion-in-zero-gravity

INTECH
open science | open minds

InTech Europe
University Campus STeP Ri
Slavka Krautzeka 83/A
51000 Rijeka, Croatia
Phone: +385 (51) 770 447
Fax: +385 (51) 686 166
www.intechopen.com

InTech China
Unit 405, Office Block, Hotel Equatorial Shanghai
No.65, Yan An Road (West), Shanghai, 200040, China
中国上海市延安西路65号上海国际贵都大饭店办公楼405单元
Phone: +86-21-62489820
Fax: +86-21-62489821